
LEARNING SUMMARY STATISTICS FOR BAYESIAN INFERENCE WITH AUTOENCODERS

Carlo Albert

Swiss Federal Institute of Aquatic
Science and Technology, Switzerland
carlo.albert@eawag.ch

Simone Ulzega

Zurich University of Applied
Sciences, Switzerland

Firat Ozdemir, Fernando Perez-Cruz

Swiss Data Science Center,
Switzerland

Antonietta Mira

Università Svizzera italiana, Switzerland
University of Insubria, Italy

ABSTRACT

For stochastic models with intractable likelihood functions, approximate Bayesian computation offers a way of approximating the true posterior through repeated comparisons of observations with simulated model outputs in terms of a small set of summary statistics. These statistics need to retain the information that is relevant for constraining the parameters but cancel out the noise. They can thus be seen as thermodynamic state variables, for general stochastic models. For many scientific applications, we need strictly more summary statistics than model parameters to reach a satisfactory approximation of the posterior. Therefore, we propose to use the inner dimension of deep neural network based Autoencoders as summary statistics. To create an incentive for the encoder to encode all the parameter-related information but not the noise, we give the decoder access to explicit or implicit information on the noise that has been used to generate the training data. We validate the approach empirically on two types of stochastic models.

Keywords Bayesian inference · Autoencoder · Thermodynamic state variables

1 Introduction

Mechanistic models are indispensable tools in many fields of research. For reliable predictions, they need to include the dominant sources of uncertainty in the form of adequate noise terms. The resulting *stochastic models* often depend on few parameters that need to be calibrated to observed data. For a probabilistic interpretation of the predictions, it is convenient to adopt the *Bayesian framework* and express our knowledge (or belief) about those parameters in terms of probability distributions. Within this framework, calibration means getting hold of the whole *posterior distribution* of parameters, expressing the combination of prior knowledge and knowledge gained from the observations, which is typically a hard *inverse problem*.

Standard algorithms for sampling from the posterior (such as the family of *Metropolis algorithms*) require a large number of evaluations of the *likelihood function*, expressing the probability density for given observed data, as a function of the model parameters. For all but trivial stochastic models, likelihood evaluations are typically prohibitively expensive as they require a high-dimensional integration over model realizations, either because the model has a large number of unobserved (latent) variables or because the normalizing partition function of the model is unknown (think, e.g., of an Ising-type model). A recent solution is to approximate the posterior by means of *neural density estimators* [Papamakarios and Murray, 2016, Papamakarios et al., 2019]. However, this requires a parametrization of the space of approximating densities, which may lead to biases that are hard to control.

Here, we take the approach of *Approximate Bayesian Computation* (ABC, e.g., [Tavaré et al., 1997, Marin et al., 2012]) - an approximate *sampling* method that is a promising alternative to variational methods if model-simulations are *fast* and parameters are *few*. ABC avoids evaluating the likelihood function, by simulating a large number of model realizations,

for various parameter sets, and accepting or rejecting those sets depending on whether or not the simulated data agrees with the observed data in terms of a given set of *summary statistics*, and within a given *tolerance*. For ABC to be accurate and efficient, we need summary statistics that, respectively, retain most of the parameter-related information and cancel out most of the noise. The latter requirement entails that summary statistics are well-concentrated, for fixed parameter values, which allows for a fast annealing of the tolerance [Albert et al., 2014].

Obvious candidates for such statistics are *parameter estimators*, such as the maximum likelihood estimator (MLE). Hence, several methods for finding summary statistics are based on *parameter regression* (e.g., [Fearnhead and Prangle, 2012, Jiang et al., 2017, Wqvist et al., 2019]). Parameter estimators are constraining the *location* of the posterior, but not necessarily its *shape*. If the data consists of a large number of independent sample points, the posterior is typically well concentrated around the true parameter values, in which case parameter estimators are near-sufficient, i.e. they contain nearly all the information that is relevant for constraining the posterior. However, in many scientific applications, we only have few realizations (e.g. from a lab experiment) or even just one (e.g. from a field experiment). And although such data sets may consist of many components (e.g. time series), they may be highly correlated. Therefore, models describing such data might produce rather different realizations, even for a *fixed* set of parameter values, and the corresponding posteriors might look rather different as well. In such situations, additional statistics may be required to reach a satisfactory approximation of the posterior.

In order to capture those additional statistics, we suggest to combine regression with reconstruction, i.e. to use neural networks of *Autoencoder-type*. Recently, Autoencoders have been employed to learn *order parameters* [Wetzel, 2017] or *collective variables* [Bonati et al., 2020], which are quantities capable of discriminating between different kinds of behavior of statistical-mechanics models. However, in order to use Autoencoders for the purpose of ABC, we have to modify them such that they encode only the features that carry information about the parameters, but not the noise. Our approach is an alternative to information-theoretic machine learning algorithms such as the ones recently presented in [Cvitkovic and Koliander, 2019] and [Chen et al., 2021].

2 Summary Statistics

Consider a generic stochastic model, defined by a conditional probability density, $f(\mathbf{x}|\boldsymbol{\theta})$, where $\boldsymbol{\theta} \in \mathbb{R}^p$ is a (low-dimensional) parameter vector and $\mathbf{x} \in \mathbb{R}^N$ a (high-dimensional) output vector. Furthermore, consider a map, $\mathbf{s} : \mathbb{R}^N \rightarrow \mathbb{R}^q$, of *summary statistics*, where q is small (of the order of p). We require \mathbf{s} to be *asymptotically sufficient*, meaning that

$$I(\boldsymbol{\Theta}, \mathbf{S}) := I(\boldsymbol{\Theta}, \mathbf{s}(\mathbf{X})) = I(\boldsymbol{\Theta}, \mathbf{X}) + \mathcal{O}(1/N), \quad (1)$$

where I denotes the *mutual information* between dependent random variables. Here, $\boldsymbol{\Theta}$ is the parameter prior with given density $f(\boldsymbol{\theta})$ and, for given $\boldsymbol{\theta}$, $\mathbf{X} \sim f(\mathbf{x}|\boldsymbol{\theta})$. Eq. (1) means that, for large data sets, the summary statistics contain almost as much information about the parameters as the whole data set. Furthermore, for ABC to converge efficiently, we require the summary statistics to cancel the noise contained in model-outputs; i.e., we require the *asymptotic concentration property*

$$H(\mathbf{S}|\boldsymbol{\Theta}) := - \int f(\mathbf{s}|\boldsymbol{\theta}) f(\boldsymbol{\theta}) \ln(f(\mathbf{s}|\boldsymbol{\theta})) d\mathbf{s} d\boldsymbol{\theta} = \mathcal{O}(1/N), \quad (2)$$

which is an asymptotic minimal entropy condition. Due to the identities

$$I(\boldsymbol{\Theta}, \mathbf{S}) = H(\mathbf{S}) - H(\mathbf{S}|\boldsymbol{\Theta}), \quad (3)$$

$$I(\boldsymbol{\Theta}, \mathbf{X}) = H(\boldsymbol{\Theta}) - H(\boldsymbol{\Theta}|\mathbf{X}), \quad (4)$$

where H denotes the entropy, we derive from conditions (1) and (2) the *asymptotic minimality*

$$H(\mathbf{S}) = H(\boldsymbol{\Theta}) + \mathcal{O}(1/N), \quad (5)$$

if we assume that the posterior is asymptotically concentrated, i.e. $H(\boldsymbol{\Theta}|\mathbf{X}) = \mathcal{O}(1/N)$.

The asymptotic sufficiency and concentration properties allow us to draw an analogy between summary statistics and *thermodynamic state variables*. As already pointed out by [Mandelbrot, 1962], the *energy* of a statistical mechanics system in equilibrium can be seen as a minimal sufficient statistic for its *temperature*. The well-known equivalence of the canonical and the micro-canonical ensembles in the thermodynamic limit is then a consequence of the concentration property. Extending this analogy a bit further, we define the *free energy*

$$F_{\boldsymbol{\theta}}(\mathbf{s}) := - \ln \int f(\mathbf{x}|\boldsymbol{\theta}) d\Omega_{\mathbf{s}}(\mathbf{x}), \quad (6)$$

where $\Omega_{\mathbf{s}}(\mathbf{x})$ is the surface measure on the shell $\mathbf{s}(\mathbf{x}) = \mathbf{s}$. If (2) is satisfied, we might expect $F_{\boldsymbol{\theta}}(\mathbf{s})$ to have a sharp minimum, for any given $\boldsymbol{\theta}$, if N is large. In that case, the prior distribution of \mathbf{S} is concentrated around a p -dimensional

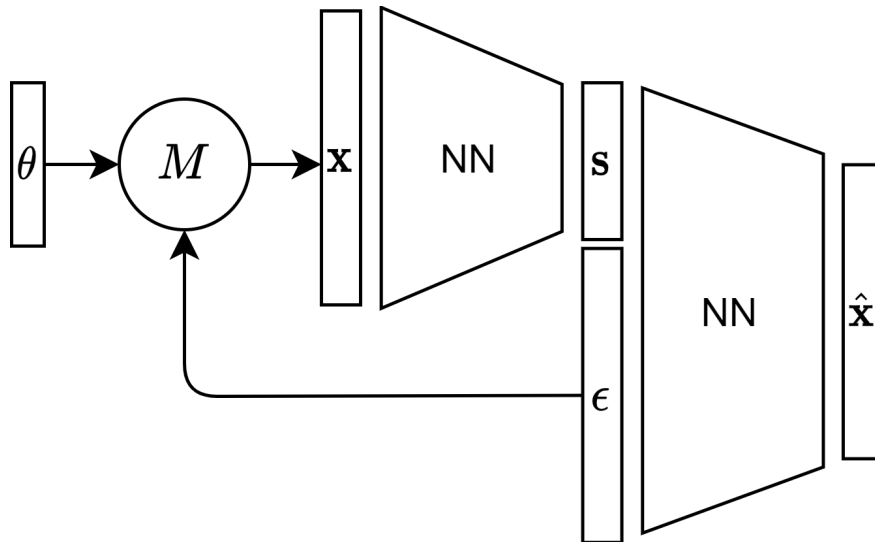


Figure 1: Basic ENCA architecture: The stochastic model needs to be available in the form of a deterministic function, M , of a parameter vector θ and a (bare) noise realization ϵ . The encoder is trained on model realizations \mathbf{x} , and produces summary statistics $\mathbf{s}(\mathbf{x})$. The decoder is trained to reproduce the model realizations $\hat{\mathbf{x}}(\mathbf{s}, \epsilon)$, based on \mathbf{s} and the same noise realizations that have been used by M . Layers within encoder and decoder neural network (NN) blocks can be optimized based on the prior knowledge about M .

submanifold in \mathbb{R}^q , and it is possible to reach a good approximation of the posterior with $q = p$ appropriately chosen summary statistics. However, even for large N , certain features that carry information about θ may not be well concentrated (due to correlations), or may exhibit more than one mode. These modes may even persist in the limit as $N \rightarrow \infty$, in which case the model exhibits different *phases*. In fact, when many non-linearly interacting degrees of freedom are present, non-trivial free energy landscapes are to be expected due to a complicated interplay between energetic and entropic terms. For such models, \mathbf{S} does not concentrate around a p -dimensional submanifold, and we need $q > p$ summary statistics, for a good posterior approximation.

3 Modified Autoencoders

We want to design Autoencoders implementing both the asymptotic sufficiency criterion (1) as well as the concentration property (2). The *encoder*, $\mathbf{s}(\mathbf{x})$, is supposed to learn the summary statistics. The first p of the q summary statistics are regularized to be parameter regressors, whereby the concentration property is implemented. The auxiliary $q - p$ summary statistics are meant to capture additional information required for constraining the posterior. The *decoder* is fed with the vector \mathbf{s} and, in addition, with either explicit or implicit information on the noise that went into generating the training data, and is supposed to either reconstruct the model outputs or the parameter values. In this manner, the encoder is incentivized to encode all the parameter-related information (sufficiency), but not the noise (concentration). The first architecture we propose (Fig. 1) has a decoder that attempts to reconstruct the model output \mathbf{x} . For this architecture, the stochastic model needs to be set up as a deterministic function, $\mathbf{x} = M(\theta, \epsilon)$, where the bare noise ϵ is sampled from a θ -independent distribution. The decoder is then given the *explicit* noise realizations ϵ that went into the generation of the training data and attempts to reconstruct the model output, i.e. it learns a function $\hat{\mathbf{x}}(\mathbf{s}, \epsilon)$. We refer to this architecture as the Explicit Noise Conditional Autoencoder (ENCA). The decoder will not only have to learn the model equations but implicitly also the reconstruction of the true parameter values θ from \mathbf{s} and ϵ (to the extent possible). For the loss function, we use the weighted sum of squares

$$\mathcal{L} = \frac{1}{p} \sum_{\alpha=1}^p \left(\frac{s_{\alpha} - \theta_{\alpha}}{\theta_{\alpha}} \right)^2 + \frac{1}{N} \sum_{i=1}^N \left(\frac{\hat{x}_i - x_i}{x_i} \right)^2. \quad (7)$$

The second architecture (Fig. 2) does not require a separation of bare noise, and is therefore more broadly applicable. It provides *implicit* information on the noise to the decoder in the form of replica of summary statistics encoded from different realizations of the model for *fixed* parameter values. That is, for a given set of parameter values θ , we generate n realizations, $\mathbf{x}^{(j)}$, for $j = 1, \dots, n$, from $f(\mathbf{x}|\theta)$, which are then passed individually onto the encoder to predict

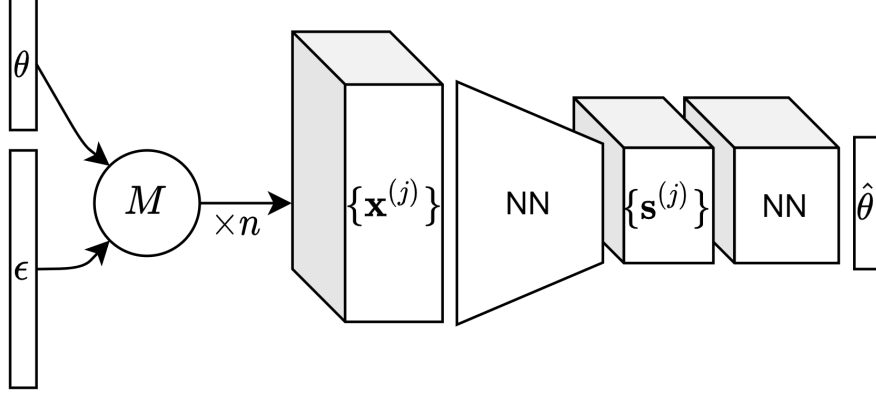


Figure 2: Basic INCA architecture: The encoder is trained on sets of model realizations $\{\mathbf{x}^{(j)}\}$, for fixed parameter values, and produces the corresponding sets of summary statistics $\{\mathbf{s}^{(j)} = \mathbf{s}(\mathbf{x}^{(j)})\}$. The decoder is a NN acting on auxiliary summary statistics $\{s_\beta^{(j)}\}$, for $\beta = p+1, \dots, q$ to find a weighting function w to reconstruct model parameters, based on eq. (8).

n summary statistics $\mathbf{s}^{(j)} = \mathbf{s}(\mathbf{x}^{(j)})$. The decoder attempts to aggregate this information into reconstructions of the parameters, $\hat{\boldsymbol{\theta}}(\{\mathbf{s}^{(j)}\})$. We refer to this architecture as the Implicit Noise Conditional Autoencoder (INCA). If we again regularize the first p components of \mathbf{s} to be parameter regressors, we can set

$$\hat{\theta}_\alpha(\{\mathbf{s}^{(j)}\}) = \frac{\sum_{j=1}^n w(\mathbf{s}^{(j)}) s_\alpha^{(j)}}{\sum_{j=1}^n w(\mathbf{s}^{(j)})}, \quad \alpha = 1, \dots, p, \quad (8)$$

where $w(\cdot)$ is a nonlinear function to be learned by the decoder based on the auxiliary summary statistics $\{s_\beta^{(j)}\}$, for $\beta = p+1, \dots, q$. If the parameter posterior strongly depends on the particular realization $\mathbf{x}^{(j)}$, for a fixed set of parameters $\boldsymbol{\theta}$, the reliability of the associated parameter regressors $s_\alpha^{(j)}$, for $\alpha = 1, \dots, p$, will also strongly depend on the particular realization j , which should be accounted for with the weights. This is precisely how the decoder incentivizes the encoder to use the auxiliary summary statistics to encode the extra features that distinguish these different realizations. As the loss function we use

$$\mathcal{L} = \sum_{j,\alpha} \left(\frac{s_\alpha^{(j)} - \theta_\alpha}{\theta_\alpha} \right)^2 + \sum_\alpha \left(\frac{\hat{\theta}_\alpha - \theta_\alpha}{\theta_\alpha} \right)^2. \quad (9)$$

4 Results

We demonstrate our method with two types of stochastic iterative map models, for which we have access to the true posterior. The first one is given by the equation

$$x_{n+1} = \alpha f(x_n) + \sigma \epsilon_n, \quad \epsilon_n \sim \mathcal{N}(0, 1) \quad \text{i.i.d.}, \quad (10)$$

where $f(x)$ is a nonlinear function admitting two stable solutions, e.g. $f(x) = x^2 e^{-x}$. The deterministic map has a stable fixed point at $x = 0$. For sufficiently large α , a second stable fixed point emerges, which, upon further increasing α , undergoes a series of period doubling bifurcations eventually leading to chaos (see Appendix 6.2, for more details on the model). Depending on the initial condition x_0 , the deterministic map will go to either one of the two attractors. This deterministic solution is the *energetically* most favored realization as it corresponds to the zero-noise realization. For sufficiently large noise, entropic effects become more important and a bi-modal free energy surface can occur. As a member of the exponential family, the minimal number of sufficient statistics for this model is bounded. However, the parametrization not being the natural one, we need *three* summary statistics to reach sufficiency, albeit the model only

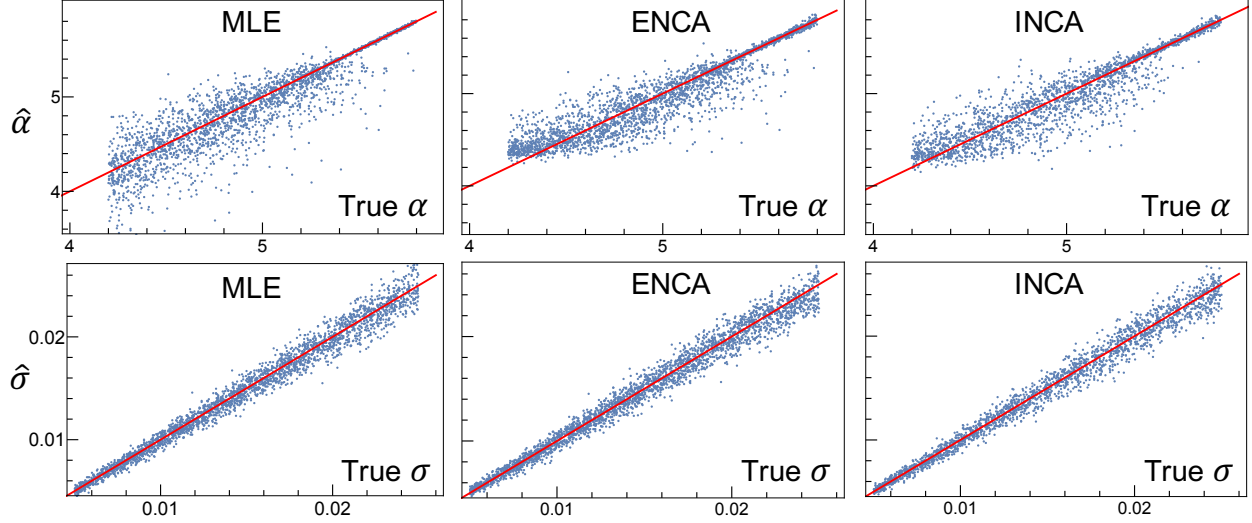


Figure 3: MLEs for the parameters of model (10) (left panels), parameter regression from the ENCA- (middle panels), and the INCA-encoder (right panels). Both ENCA and INCA are trained with $q = 3$ summary statistics. The upper row of plots shows a clear accuracy-difference for the two phases of the model.

has two parameters, $\boldsymbol{\theta} = (\alpha, \sigma)^T$. A convenient parametrization, for sufficient statistics, is given by eqs.

$$\hat{\alpha}(\mathbf{x}) = \frac{\sum_{n=1}^N x_n f(x_{n-1})}{\sum_{n=1}^N (f(x_{n-1}))^2}, \quad (11)$$

$$\hat{\sigma}(\mathbf{x}) = \frac{1}{N} \sum_{n=1}^N (x_n - \hat{\alpha}(\mathbf{x}) f(x_{n-1}))^2, \quad (12)$$

$$o(\mathbf{x}) = \frac{1}{N} \sum_{n=1}^N (f(x_{n-1}))^2. \quad (13)$$

The first two statistics are MLEs for the two parameters, inferring α from the auto-correlation and σ from the residuals, respectively. The third one, $o(\mathbf{x})$, can be seen as an *order parameter* that is needed to tell the two attractors apart. We have chosen the initial point x_0 in between the two attractors, and the prior such that the switching time between them is much longer than the observation time. Thus, there are parameter values $\boldsymbol{\theta}$, for which $F_{\boldsymbol{\theta}}(\mathbf{s})$ is bi-modal, for $\mathbf{s} = (\hat{\alpha}, \hat{\sigma}, o)^T$ (Fig. 4). For these values, the third statistic is not approximated by a function of the other two. Hence it contains information about the parameters that is not contained in the other two statistics. Fig. 3 shows that apart from prior boundary effects, both architectures yield parameter regressors (first two components of \mathbf{s}) that are very similar to MLEs (first two components of the sufficient summary statistics (11), (12)). In order to accurately reconstruct the output, the decoder of both ENCA and INCA forces the encoder to also learn a quantity equivalent to the third statistic, although INCA separates the two “phases” less clearly (Fig. 4). Fig. 5 compares ABC-posteriors, for different sets of summary statistics, against a posterior-sample generated with a Metropolis algorithm. Using the encoder-generated summary statistics from the two architectures confirms that both are near-sufficient, albeit the approximate posterior achieved with INCA is a bit less accurate; i.e., wider. Both approximate posteriors are much closer to the true posterior compared to the approximate posterior we get when we only use the two MLE regressors (11) and (12). Hence, our Autoencoder-generated summary statistics will outperform any statistics generated by machine-learning models that are solely based on parameter regression.

The second example is a stochastic non-linear iterative map model with both additive and multiplicative noise:

$$x_{i+1} = \alpha_i f(x_i) + \epsilon_i, \quad \alpha_i \sim \mathcal{U}[\alpha, \alpha + \delta], \quad \epsilon_i \sim \mathcal{U}[0, \epsilon] \quad \text{i.i.d.} \quad (14)$$

and three parameters, $\boldsymbol{\theta} = (\alpha, \delta, \epsilon)^T$. It is an example for the common situation where we have more internal-noise degrees of freedom ($\boldsymbol{\alpha}, \boldsymbol{\epsilon}$) than observed output components (\mathbf{x}). Integrating out the unobserved degrees of freedom typically takes us outside of the exponential family, as is the case for this model. Consequently, we would need to use the entire data-set ($q = N$) to achieve strict sufficiency. However, we expect to be able to compress most of the parameter-related information into few summary statistics nonetheless. We have trained both ENCA and INCA with 3

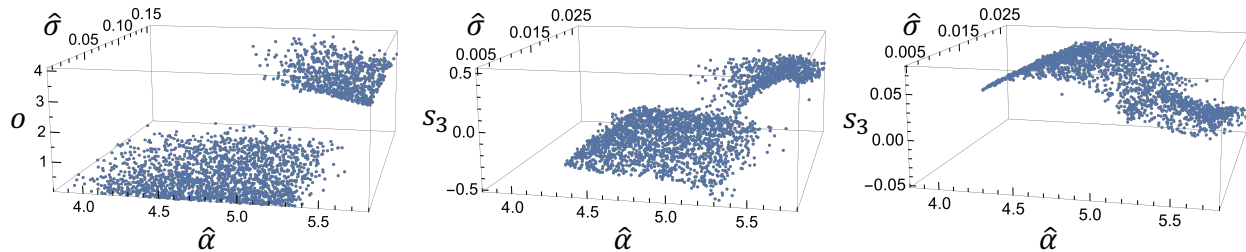


Figure 4: Prior distribution of sufficient summary statistics (11) - (13) (left), and of the latent variables from both ENCA (middle) and INCA (right). The two sheets correspond to the two attractors of the model and overlap on the $(\hat{\alpha}, \hat{\sigma})$ -projection (bi-modality).

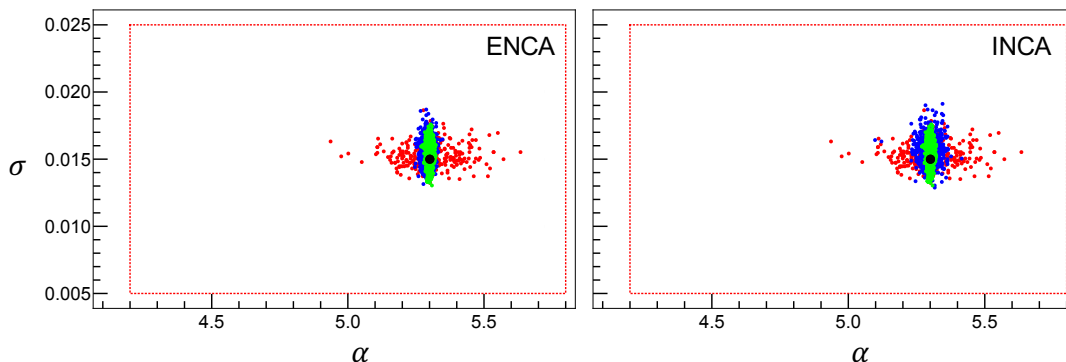


Figure 5: Metropolis-generated posterior for model (10) (green) compared against ABC posteriors using all three latent variables (blue) from ENCA (left) and INCA (right) and using only the two regressors (red). The dashed boxes represent the ABC priors, while the black dots represent the true values of the parameters used to generate the synthetic data set.

($q = p$) as well as 4, 5 and 6 summary statistics. Fig. 6 shows that, when training ENCA on model (14), adding a fourth statistic has a small yet noticeable effect on the first statistic, i.e. the regressor for α . This means that the decoder can facilitate the regression of the encoder, but its main purpose is to create the incentive to encode additional information in the auxiliary statistics. That it does so indeed is shown in Fig. 7. When using only 3 statistics the decoder does not manage to reconstruct the model output, but with only 4 the reconstruction is almost perfect. Correspondingly, using 4 or 5 statistics leads to approximate posteriors that are more accurate than the one achieved with only 3 statistics. (Fig. 8). Using more than 5 statistics leads to a degradation of the ABC-posterior. Presumably this is because the statistics start to encode more of the noise, which degrades their concentration. Similarly, the approximate posteriors resulting from INCA-generated summary statistics are most accurate when using 5 statistics (Fig. 9).

When deciding about the optimal number of statistics (when the true posterior is not known) the distances to the observations achieved with ABC can be an indication (Fig. 10). According to eq. (3), large distances (lack of concentration) can be the result of either too few statistics (lack of sufficiency) or too many (lack of minimality). The posterior accuracy achieved with ENCA is in line with the achieved ABC distances. Although with INCA the smallest distances are achieved with 3 statistics, the posterior with 5 statistics is marginally better. This is the case because, for dimensional reasons, the lower the number of statistics the smaller the distances tend to be.

5 Conclusions

We have given a proof of concept that Autoencoder-like architectures providing additional noise-information to the decoder can be used to learn summary statistics that are both near-sufficient and highly concentrated - two criteria that are required for ABC to work both accurately and efficiently. While the decoder can help the encoder to find good parameter regressors, its main job is to create an incentive for encoding additional information that is relevant for constraining the parameters. We have proposed two types of decoders, one that attempts to reconstruct the outputs and is given explicit noise information, and one that attempts to reconstruct the parameters and is given implicit noise information. In our case studies, the former achieved slightly better results, whereas the latter has a broader range of applicability. For the proof of concept we have chosen members of two types of nonlinear stochastic models. The first

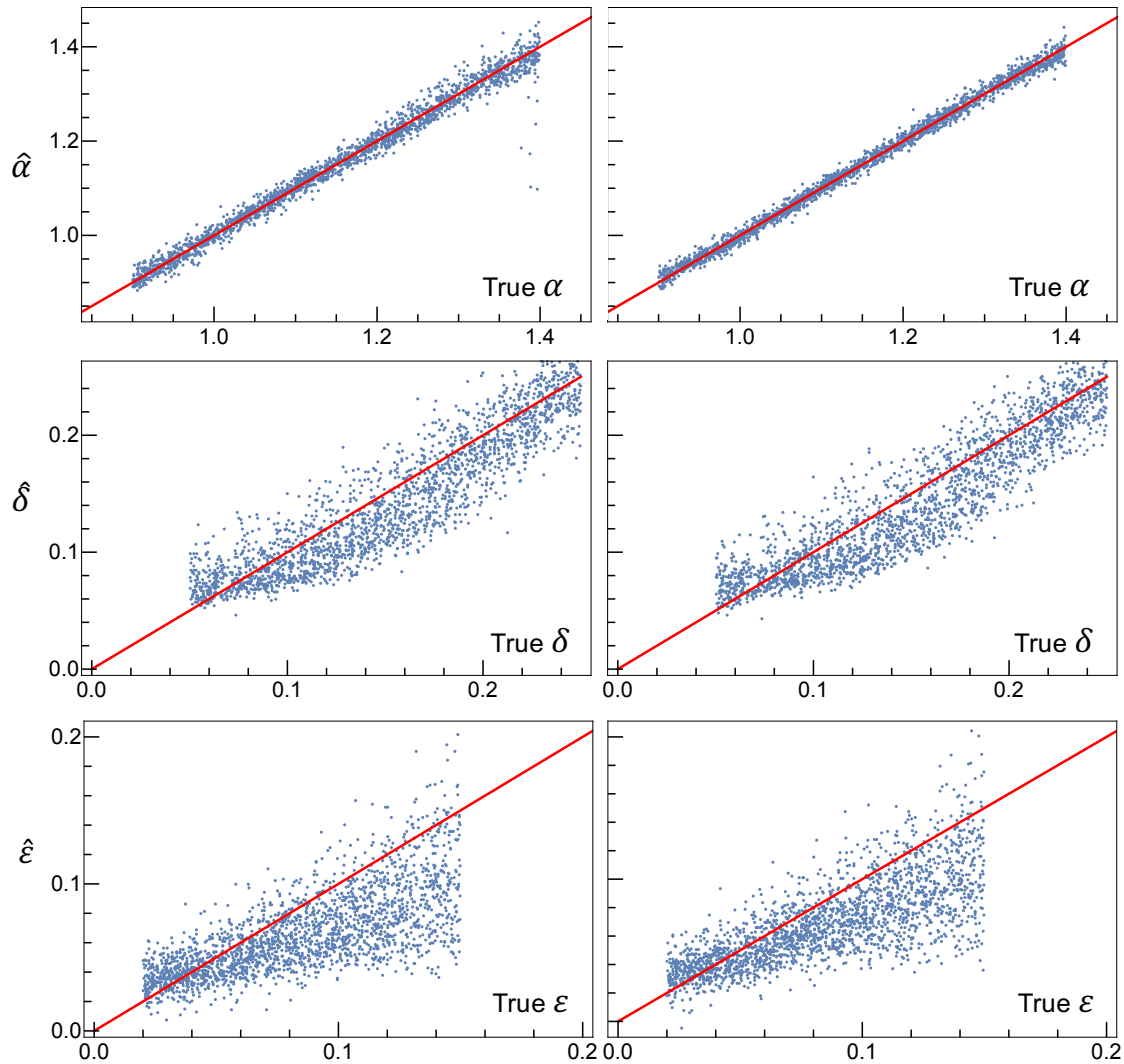


Figure 6: Parameter regression for model (14) from ENCA, using three (left column) or four (right column) latent variables. The contribution of the additional feature to the α -marginal is small but noticeable. (Results are similar for INCA.)

model is a member of the exponential family, which allowed us to compare the learned summary statistics against a known set of sufficient statistics. This model also exemplifies that stochastic nonlinear models can exhibit different “phases”, which might require us to use more summary statistics than parameters. The second model is an example for the common situation where we have more internal-noise degrees of freedom than observed output components, and lies outside of the exponential family, where no bounded set of sufficient statistics is available. Nevertheless, in our example we show that a very good approximation of the true posterior can be achieved with ABC with a small number of learned summary statistics that is, once again, larger than the number of parameters. As a criterion for the optimal number of summary statistics we suggest to use the distances between simulated and observed summary statistics achieved within ABC.

Our methods are applicable to a large range of stochastic models that allow for cheap forward simulations. However, we present only a proof of concept. More research is required to explore and validate their applicability in practical applications.

The summary statistics generated by our methods are of interest beyond Bayesian inference and should be seen within the larger context of *feature learning*. In particular, our method can also be applied to observed instead of model-generated data, and is applicable whenever we want to disentangle low-dimensional relevant features from high-dimensional irrelevant (noise) features.

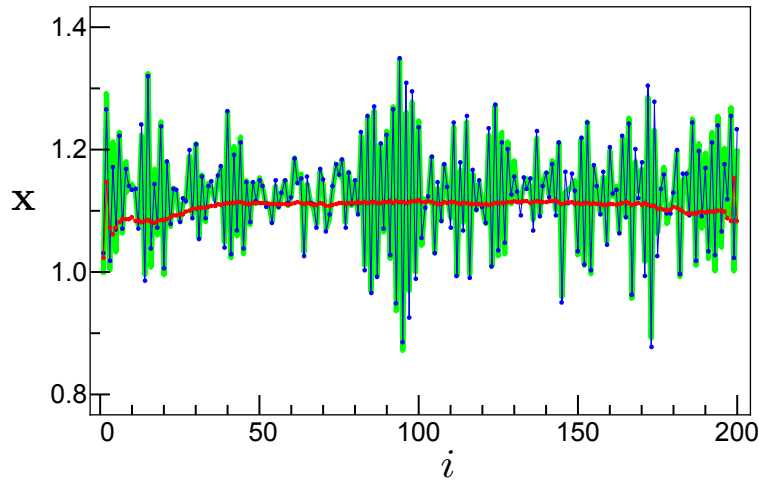


Figure 7: Typical time-series x generated by model (14) (green) compared against the reconstruction by the ENCA-decoder, using three (red) or four (blue) latent variables. The contribution of the additional statistic is indisputable.

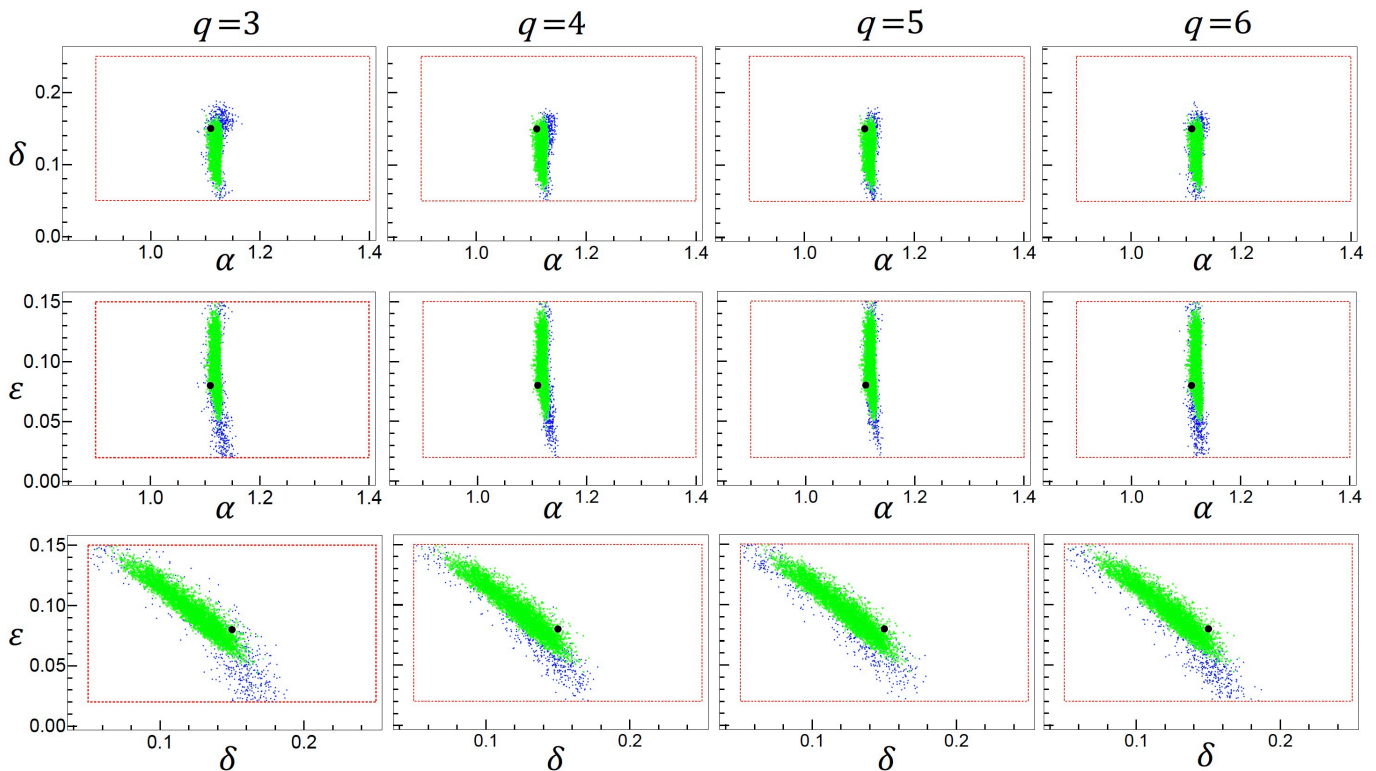


Figure 8: 2D projections of the true posterior for model (14) (green) compared against ABC posteriors (blue) from ENCA using, from left to right columns, three, four, five and six summary statistics ($q = 3, 4, 5, 6$). The dashed boxes represent the ABC priors, while the black dots represent the true values of the parameters used to generate the synthetic data set.

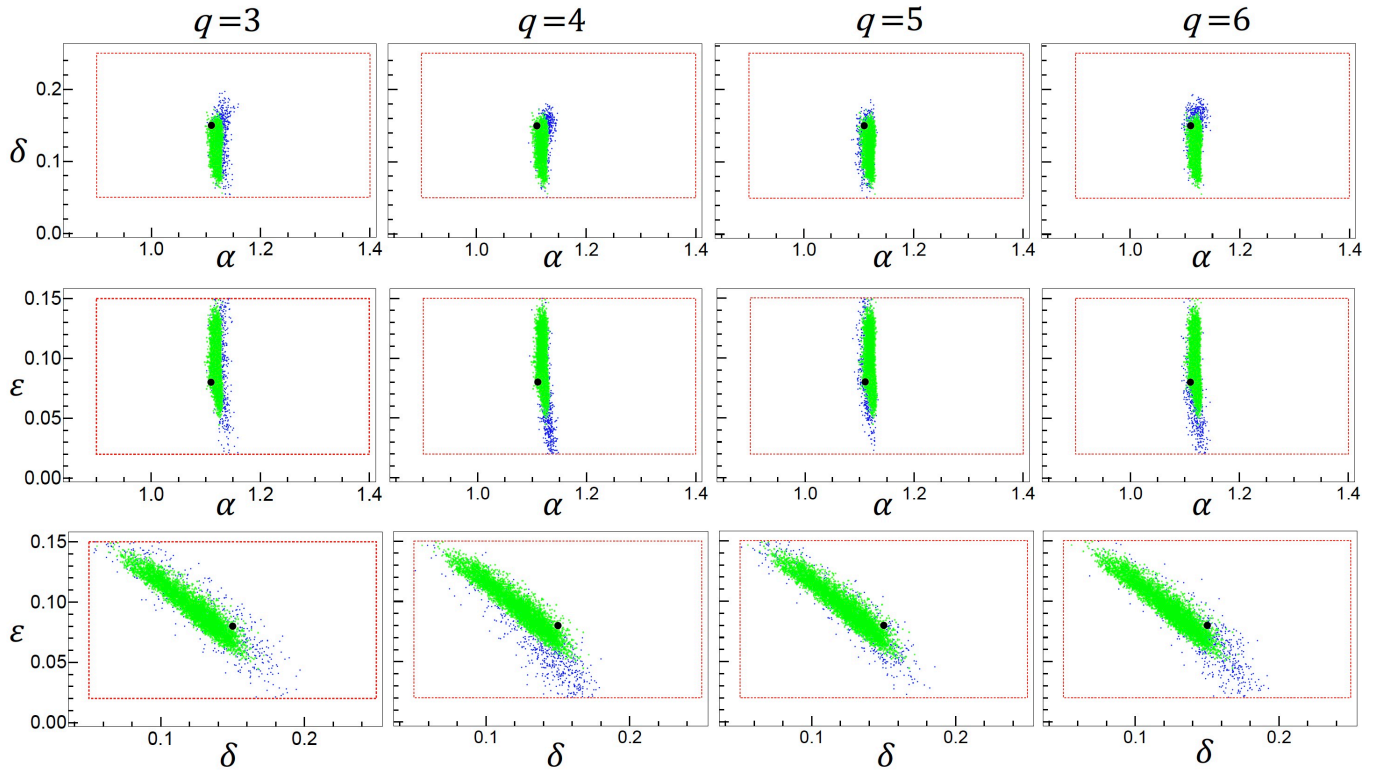


Figure 9: Analogously to Fig.8, the exact posteriors for model (14) (green) are compared against ABC posteriors (blue) from INCA.

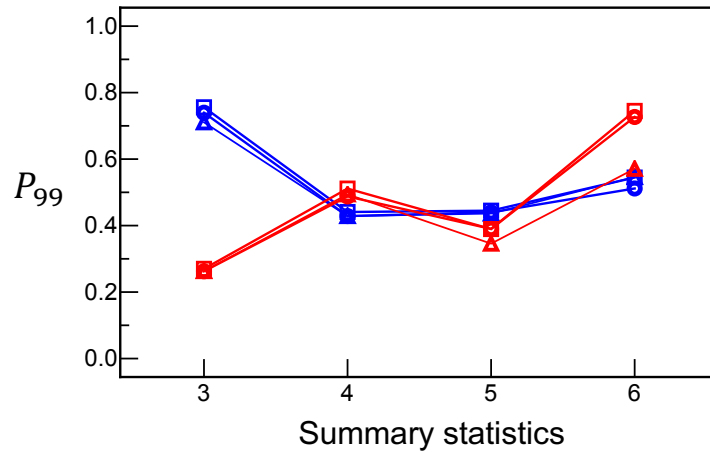


Figure 10: 99%-percentiles of the distance-distributions of the parameter regressors achieved within ABC for ENCA (blue) and INCA (red), as a function of the total number of used statistics, for model (14). Circles, squares and triangles correspond to the regressors for α , δ , and ϵ , respectively. Latent spaces of dimension 4 and 5 yield the most accurate posterior for ENCA (Fig. 8), whereas for INCA 5 summary statistics lead to the best result (Fig. 9). The full distributions are shown in the Appendix.

Acknowledgements

This work is part of the BISTOM project, funded by the Swiss Data Science Center.

6 Appendix

6.1 Implementation Details

For both INCA and ENCA, we use the same NN architecture for the encoder, which consists of only convolutional and pooling layers (see Table 1). One major difference in implementation comes from the fact that ENCA has 3 dimensional activations, (minibatch size, temporal axis, channel axis), as opposed to 4 in INCA, which has an additional dimension for the n replica. The decoder architectures for ENCA and INCA are shown in Tables 2 & 3. We chose a recurrent neural network architecture for the ENCA-decoder in order to estimate the input observation where we paired bare noise with summary statistics for each time step. We used a multilayer perceptron architecture to learn the mapping function $w(\cdot)$ within the INCA-decoder, which is later used as in eq. (8). For model (10), for both ENCA and INCA, we set the number of observations to 300 samples per training step; i.e., minibatch size for ENCA and $n \times$ minibatch size for INCA. For model (14) instead we set the number of observations per training step to 100 samples for ENCA, and to 300 samples for INCA. We used Adam optimizer with an initial learning rate of 10^{-3} for training both architectures.

6.2 Statistical Model Priors

We conducted our experiments for eq. (10) using the following priors: $\alpha \sim \mathcal{U}(4.2, 5.8)$, $\sigma \sim \mathcal{U}(0.005, 0.025)$, and $x_0 = 0.25$. The true values used in ABC experiments were $\alpha = 5.3$ and $\sigma = 0.015$. Throughout our experiments with the model from eq. (14), we used the following priors: $\alpha \sim \mathcal{U}(0.9, 1.4)$, $\delta \sim \mathcal{U}(0.05, 0.25)$, $\epsilon \sim \mathcal{U}(0.02, 0.15)$, and $x_0 = 1.0$. The true values used in ABC experiments were $\alpha = 1.11$, $\delta = 0.15$ and $\epsilon = 0.08$.

The choice of statistical model priors and true values in our experiments are based on the stable points, bifurcations, and chaotic regions of the test models (see Fig. 11). For model (10), the transition between the two stable fixed points, i.e., the zero and non-zero solutions, occurs at $\alpha \approx 5.3$. The parameter priors limit the region of interest to the vicinity of that point, where the two stable regimes can coexist, remaining well outside the chaotic region appearing at $\alpha \approx 5.9$. In the case of model (14), the parameter priors ensure that all regimes are taken into account, including the stable solutions, all bifurcations and the chaotic regime.

6.3 Training Resources

The training of the Autoencoders and the ABC inference were run on the internal cluster of the Zurich University of Applied Science (ZHAW, Switzerland), using for each of them a full node equipped with two 16-core 2.6-3.7 GHz processors (Xeon-Gold 6142) and 196 GB of memory. The Autoencoders were trained for a very long time to make sure that the loss function reached a plateau. That is, they were trained for about 10^6 training steps, which took about 3 (INCA) and 5 (ENCA) days for model (10), 6 (ENCA) and 11 (INCA) days for model (14).

For the ABC inference we used the simulated annealing ABC algorithm [Albert et al., 2014] as implemented in the SPUX¹ framework. Each inference took about 2 hours for $75 \cdot 10^4$ model realisations, for both models. This large

¹<https://spux.readthedocs.io>

input	layer name	hyper-parameters	output shape (ENCA)	output shape (INCA)
	observation	input	(bs, 200, 1)	(bs, n , 200, 1)
observation	conv1.1	3, 16 relu	(bs, 198, 16)	(bs, n , 198, 16)
conv1.1	conv1.2	3, 16 relu	(bs, 196, 16)	(bs, n , 196, 16)
conv1.2	maxpool	2	(bs, 98, 16)	(bs, n , 98, 16)
maxpool1	conv2.1	3, 32 relu	(bs, 96, 32)	(bs, n , 96, 32)
conv2.1	conv2.2	3, 32 relu	(bs, 94, 32)	(bs, n , 94, 32)
conv2.2	conv3	3, q , linear	(bs, 92, q)	(bs, n , 92, q)
conv3	globpool	N/A	(bs, q)	(bs, n , q)

Table 1: Encoder architectures of the ENCA and INCA models. Global average pooling layer is denoted as globpool. Convolutional layer (conv) hyper-parameters correspond to kernel size, number of filters, and activation, respectively. Output shapes are listed for observation length of 200 steps and minibatch size is denoted as bs.

Decoder ENCA			
input	layer name	hyper-parameters	output shape
summary statistics	tile \mathbf{s}	N/A	(bs, 200, q)
	ϵ	noise	(bs, 200, c_ϵ)
[tile \mathbf{s} , noise]	concatenate	N/A	(bs, 200, $c_\epsilon + q$)
concatenate	Bi-LSTM1	16, tanh	(bs, 200, 32)
Bi-LSTM1	Bi-LSTM2	16, tanh	(bs, 200, 32)
Bi-LSTM2	FC	1, linear	(bs, 200, 1)

Table 2: Decoder architecture of ENCA. Bidirectional (Bi)-LSTM layer details correspond to number of LSTM filters ($\times 2$ due to Bi) and activation, respectively. Fully connected (FC) layer details correspond to number of hidden units, and activation, respectively. Output shapes are listed for an initial observation length of 200 steps constructed using noise vector $\epsilon \in \mathbb{R}^{200 \times c_\epsilon}$ having c_ϵ channels. Minibatch size is denoted as bs. Note that c_ϵ is 1 and 2, for the two test models, respectively. Tile layer corresponds to broadcasting operation along a new axis. For more details, please refer to our repository.

Decoder INCA			
input	layer name	hyper-parameters	output shape
	$\{\mathbf{s}^{(j)}\}_{j=p+1, \dots, q}$	N/A	(bs, n , $q - p$)
$\{\mathbf{s}^{(j)}\}_{j=p+1, \dots, q}$	FC1	3, leakyReLU	(bs, n , 3)
FC1	FC2	10, leakyReLU	(bs, n , 10)
FC2	FC3	3, leakyReLU	(bs, n , 3)
FC3	FC4 (i.e., $w(\cdot)$)	1, sigmoid	(bs, n , 1)
$[w(\cdot), \{\mathbf{s}^{(j)}\}_{j=1, \dots, p}]$	Eq. (8)	N/A	(bs, p)

Table 3: Decoder architecture of INCA. Fully connected (FC) layer details correspond to number of hidden units, and activation, respectively. All leakyReLU activations have their $\alpha = 0.3$. Output shapes are listed for an initial observation length of 200 steps constructed using noise vector $\epsilon \in \mathbb{R}^{200 \times c_\epsilon}$ having c_ϵ channels. Minibatch size is denoted as bs. $\{\mathbf{s}^{(j)}\}_{j=p+1, \dots, q}$ corresponds to auxiliary summary statistics. For more details, please refer to our repository.

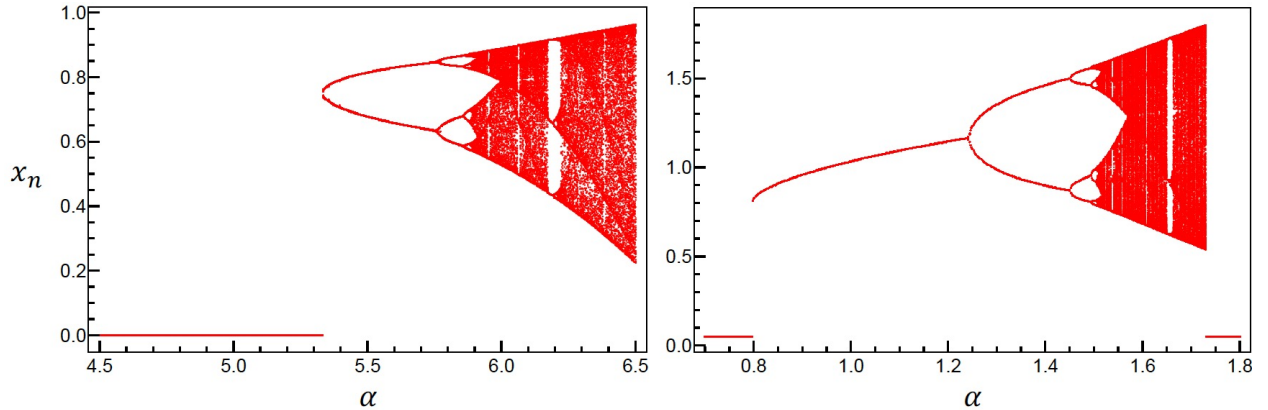


Figure 11: Amplitudes of the iterates x_n as a function of the parameter α for the deterministic part of model (10) (left) and for model (14) (right) assuming a constant α and replacing the additive noise with its average value. In both cases, one observes two stable fixed points, corresponding to zero and non-zero solutions, and the cascade of period doubling bifurcations that characterizes the route to a chaotic regime.

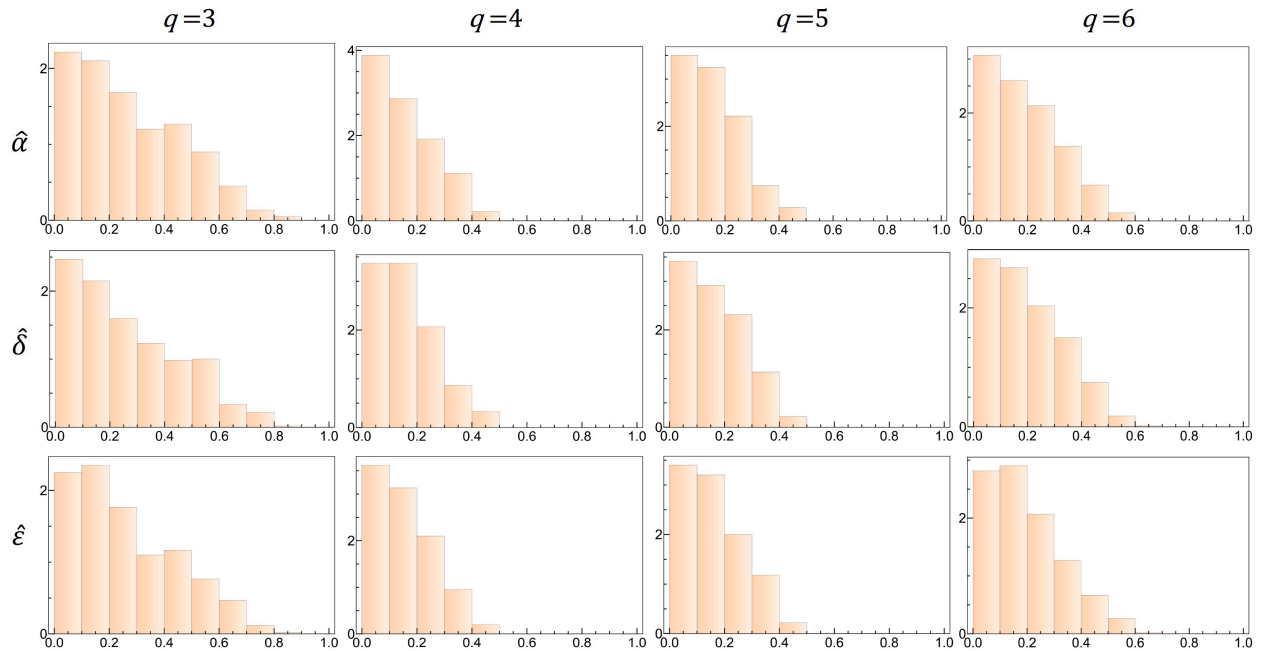


Figure 12: Histograms of the final accepted distances between observed and simulated summary statistics achieved with ABC, for model (14). Only the first three summary statistics, i.e., the parameter regressors, are plotted (rows). The columns correspond to different architectures of ENCA, that is, latent space dimensions of 3, 4, 5, or 6, as specified by the column labels.

number of model realisations ensures that the ABC-inference process practically converges, with a remaining acceptance rate of typically well below 1%.

6.4 Additional results

Figs. 12 and 13 show the full histograms of the ABC-distances, from which the quantiles in Fig. 10 in the main text were derived.

References

- [Albert et al., 2014] Albert, C., Künsch, H.-R., and Scheidegger, A. (2014). A Simulated Annealing Approach to Approximate Bayes Computations. *Stat. Comput.*, 25(6):1217–1232.
- [Bonati et al., 2020] Bonati, L., Rizzi, V., and Parrinello, M. (2020). Data-driven collective variables for enhanced sampling. *The Journal of Physical Chemistry Letters*, 11(8):2998–3004.
- [Chen et al., 2021] Chen, Y., Zhang, D., Gutmann, M. U., Courville, A., and Zhu, Z. (2021). Neural approximate sufficient statistics for implicit models. In *Ninth International Conference on Learning Representations 2021*.
- [Cvitkovic and Koliander, 2019] Cvitkovic, M. and Koliander, G. (2019). Minimal achievable sufficient statistic learning. In *International Conference on Machine Learning*, pages 1465–1474. PMLR.
- [Fearnhead and Prangle, 2012] Fearnhead, P. and Prangle, D. (2012). Constructing summary statistics for approximate Bayesian computation: semi-automatic approximate Bayesian computation. *J. Roy. Stat. Soc. B*, 74(3):419–474.
- [Jiang et al., 2017] Jiang, B., Wu, T.-y., Zheng, C., and Wong, W. H. (2017). Learning summary statistic for approximate Bayesian computation via deep neural network. *Statistica Sinica*, pages 1595–1618.
- [Mandelbrot, 1962] Mandelbrot, B. (1962). The role of sufficiency and of estimation in thermodynamics. *The Annals of Mathematical Statistics*, pages 1021–1038.
- [Marin et al., 2012] Marin, J., Pudlo, P., Robert, C., and Ryder, R. (2012). Approximate Bayesian computational methods. *Statistics and Computing*, 22(6, SI):1167–1180.

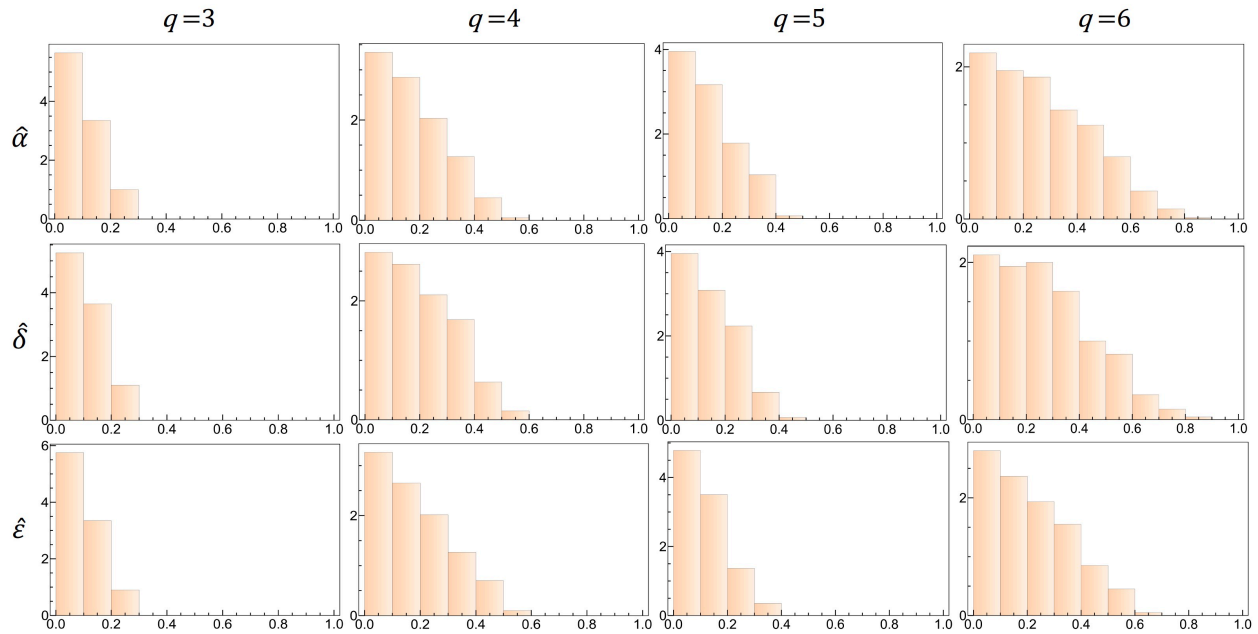


Figure 13: Distance distributions as in Fig. 12, for different architectures of INCA.

- [Papamakarios and Murray, 2016] Papamakarios, G. and Murray, I. (2016). Fast ε -free inference of simulation models with Bayesian conditional density estimation. In *NIPS*.
- [Papamakarios et al., 2019] Papamakarios, G., Sterratt, D., and Murray, I. (2019). Sequential neural likelihood: Fast likelihood-free inference with autoregressive flows. In *The 22nd International Conference on Artificial Intelligence and Statistics*, pages 837–848. PMLR.
- [Tavaré et al., 1997] Tavaré, S., Balding, D., Griffiths, R., and Donnelly, P. (1997). Inferring Coalescence Times From DNA Sequence Data. *Genetics*, 145:505–518.
- [Wetzel, 2017] Wetzel, S. J. (2017). Unsupervised learning of phase transitions: From principal component analysis to variational autoencoders. *Physical Review E*, 96(2):022140.
- [Wiqvist et al., 2019] Wiqvist, S., Mattei, P.-A., Picchini, U., and Frellsen, J. (2019). Partially exchangeable networks and architectures for learning summary statistics in approximate Bayesian computation. In *International Conference on Machine Learning*, pages 6798–6807. PMLR.